



Science Arts & Métiers (SAM)

is an open access repository that collects the work of Arts et Métiers Institute of Technology researchers and makes it freely available over the web where possible.

This is an author-deposited version published in: <https://sam.ensam.eu>
Handle ID: <http://hdl.handle.net/10985/7465>

To cite this version :

Anna Carla ARAUJO, Guillaume FROMENTIN, Gerard POULACHON - Analytical and experimental investigations on thread milling forces in titanium alloy - International Journal of Machine Tools and Manufacture - Vol. 67, p.28-34 - 2013

Any correspondence concerning this service should be sent to the repository

Administrator : scienceouverte@ensam.eu



Analytical and experimental investigations on thread milling forces in Titanium Alloy

Anna Carla Araujo¹, Guillaume Fromentin² and Gérard Poulachon²

1 - COPPE/UFRJ

2 - LABOMAP-ENSAM

Abstract

This study deals with thread milling process that it is considered a complex machining technique due to its elaborated tool geometry and its tridimensional tool trajectory. It is needed advanced research on the threading process which has not been much studied. Previous studies focused on geometrical modeling or mechanistic modeling of the thread milling process. There is a need of a better understanding of parameter effects to accomplish a model that tends to be more realistic and includes local parameters. This investigation does the analysis of thread milling parameters: thread geometry, cutting conditions and tool angles, which can be applied to the tool optimization. The cutting forces and torque were measured and representative values of its variation were calculated and analyzed as response of the experiments. A geometrical analysis and an analysis of variance were employed for determining the influence of the factors and based on the results, it is proposed a physical understanding of the process.

Keywords: Thread milling, Titanium alloy, Cutting forces and Design of experiments.

1 Introduction

Threaded pieces are needed for wide applications in industry and it can be manufactured in a variety of ways, applying the two basic principles: plastic working or metal cutting. Threads produced by plastic deformation have higher strength than the machined ones, but does not guarantee high accuracy or precision as in tapping and thread milling, the cutting methods. Specially for brittle or special materials which cannot be produced by plastic working.

As an example, materials for medical solutions, as titanium alloys and smart material alloys, requires manufacturing process with controlled proprieties and precision either for internal and external threads. There are very few papers exploring thread milling forces on titanium alloys although it is been widely used for medical and dental implants [Malaguti et al., 2011], [Lopez-Heredia et al., 2008] e [Yamazoe, 2010].

Internal thread cutting can be produced by tapping tools in machining center or by turning tools in lathe, in these cases feed velocity can be very high because it is proportional to the thread pitch, cutting velocity and tool diameter. Breakage of a thread-cutting tool can impact significantly the productivity of the process [Veldhuis et al., 2007]. When compared to form tapping [Fromentin et al., 2005] or cut tapping, a broken tool in thread milling is easier to evacuate without damaging the workpiece, so it is a good alternative for high cost parts. While tapping requires

a given tool for producing an specific thread dimension, thread milling can produce threads in bigger diameters and special threads.

For cut tapping there are some researchers dedicated to develop models for the process: mechanistic models for the prediction of tapping torque including identification of faults typical of a tapping operation (as misalignment, runout and tooth breakage); [Cao and Sutherland, 2002] e [Mezentsev et al., 2002], unified-generalized mechanics of cutting model, as it is called on [Armarego and Chen, 2002], and experimental studies, as in [Li et al., 2003] that used the electrical current signal of the spindle motor for diagnosis.

The study on thread milling cutting forces was first developed by Araujo *et al* [Araujo et al., 2006]. A mechanistic force model was created from a linear thread cutting experiment where the referential frames were superposed and independent from the tool trajectory. The feed velocity in vertical direction was neglected. After mechanistic calibration, the model was applied in helical path by rotating force basis and it was validated. Fromentin *et al.* in 2010, [Fromentin and Poulachon, 2010a] and [Fromentin and Poulachon, 2010b], developed a geometric local analysis for thread milling considering the envelope tool profile, an analytical formulation of the cutting edges and a more precise calculation for uncut chip thickness. It is pointed out a concern on interesting local cutting edge aspects, including flute angle, and how it reflects on the cutting area and cutting force components. The present study includes some changes on geometrical analysis if it is compared to the previous ones [Fromentin and Poulachon, 2010b]. Those geometrical and phenomenological hypothesis have to be validated by experimental analysis.

In 2012, Sharma *et al.* [Sharma et al., 2012] developed a model adding the vertical feed to the simulation. Another important improvement in the force model concerns on the calibration that takes into account local normal rake angle in the cutting edge is considered [Fromentin and Poulachon, 2010b].

The technique of designs of experiments (DOE) and analysis of variance (ANOVA) is widely used to optimize parameters of machining processes due to its capacity to identify the most influential factors on the process, as presented in [Yang et al., 2009] and [Ghani et al., 2004] for end milling analysis.

The main goal of this article is to achieve the understanding of global forces, based on experiments and its relation to geometrical parameters. The present study is focused on the thread milling of titanium alloy Ti6Al4V and the following parameters are studied: flute angle, rake angle, thread diameter, depth of cut and feed rate. A geometrical analysis is presented and it defines criteria to characterize the thread milling conditions. A specific experimental set-up was developed for measuring cutting force, acquiring tool position and computing forces in different referential frames needed for mechanical analysis. From data analysis the article proposes some modifications on its analysis and it opens further possibilities for tool optimization and mechanistic force modeling.

2 Process Analysis

The basics of thread milling processes and tool sequences are described in previous articles [Araujo et al., 2006, Sharma et al., 2012, Araujo et al., 2004, Araujo and Jun, 2009].

The thread machining begins positioning the tool on the center of a drilled hole, followed by a penetration strategy to the bulk. There are basically three penetration strategies [Fromentin et al., 2011]: straight penetration, quarter revolution penetration and half revolution penetration (HRP), which is used in Figure 1a of the present article. After the penetration, the tool is said to be in “full machining” (FM) and the tool axis trajectory describes a r_{tt} radius circle in the XY projection plane inside the drilled hole. The internal threads studied in this article are metrical, right hand, one tool pass is used and the cutting begins with the tool in the lower part of the hole, ending in the top after producing the helical trajectory. The total tool displacement in FM for z is one thread pitch P [ISO, 1998]. After the cutting, the tool retracts from the thread surface to the center of the hole and after outside the workpiece.

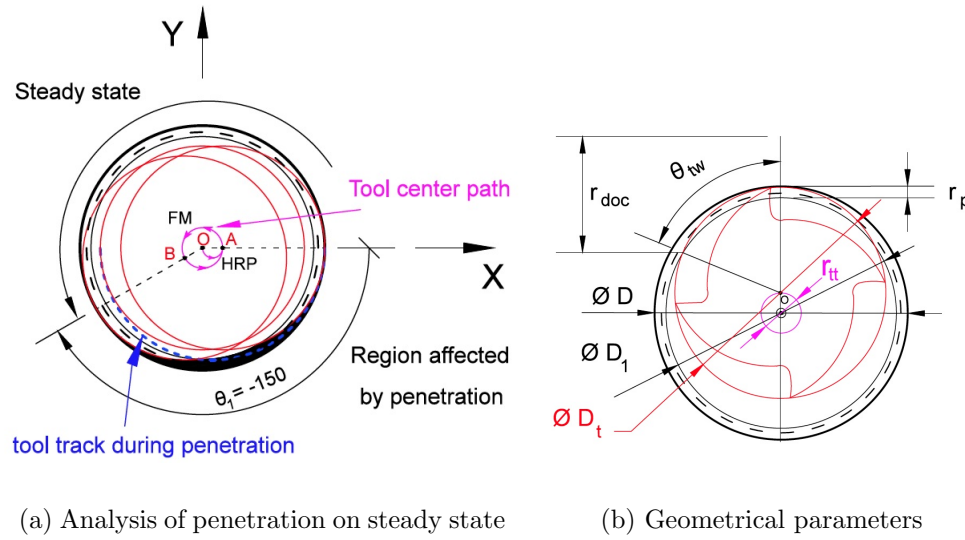


Figure 1: Thread Milling Process in Aerial View

2.1 Thread Milling Parameters

The thread milling parameters are presented in order to clarify and unify the nomenclature from published articles. In full machining, the tool has two important engagement parameters related to circular trajectory: radial depth of cut r_{doc} and radial penetration r_p , shown in Figure 1b. Radial penetration is calculated using the nominal thread diameter D and the minor diameter of the internal thread D_1 [ISO, 1998], and for the most common case is described in [Fromentin and Poulachon, 2010b] as:

$$r_p = \frac{D - D_1}{2} \quad (1)$$

For this case, the radial depth of cut is written as a function of the thread pitch and the tool diameter D_t , defined by [Fromentin and Poulachon, 2010b] by:

$$r_{doc} = \frac{P(80.\sqrt{3}D - 75.P)}{256(D - D_t)} \quad (2)$$

The instantaneous axial depth of cut a'_{doc} reduces (in FM) from initial axial depth of cut a_{doc} down to $(a_{doc} - P)$, as the tool goes up and z increases.

Feed per tooth f_t takes into account the helical trajectory used by the CNC command. It can be projected to the XY plane $f_{t_{xy}}$ and calculated as a function of the angular thread pitch $p_\theta = P/2\pi$ [Fromentin and Poulachon, 2010b]:

$$f_{t_{xy}} = \frac{f_t}{\sqrt{\left(\frac{p_\theta}{r_{tt}}\right)^2 + 1}} \quad (3)$$

For each pitch profile to be manufactured, the tool cutting edge presents three orientations: upper, front and lower cutting edge, as presented in [Fromentin and Poulachon, 2010b]. The maximum uncut chip thickness $t_{c_{max}}$ on front cutting edge has close relation to the cutting force. In thread milling it is calculated as an approximated function of the radial depth of cut and tool diameter, as in Eq. 4 [Fromentin and Poulachon, 2010b]:

$$t_{c_{max}} \approx 2f_{t_{xy}} \sqrt{\frac{r_{doc}}{D_t} \left(1 - \frac{r_{doc}}{D_t}\right)} \quad (4)$$

2.2 Cutting Continuity

Cutting continuity is an important property for end milling and thread milling that reduces the instantaneous cutting force and the amplitude of its variation that contributes for vibrations and a possible fatigue fracture. The flute angle λ_{st} contributes directly to the cutting continuity. The flute in contact with the cylindrical surface defines, in XY plane, an flute engagement angle δ , presented by Tlustý [Tlustý and MacNeil, 1975]. For end milling using constant a_{doc} , it is calculated by:

$$\delta = \frac{2a_{doc} \tan(\lambda_{st})}{D_t} \quad (5)$$

The engagement tool angle in XY plan (Figure 1b) is called tooth working angle θ_{tw} [Sharma et al., 2012]. This angle is calculated considering the r_{doc} , constant for a defined thread dimension, and D_t which has limited diameter for internal thread due to the hole dimension:

$$\theta_{tw} = \arccos\left(1 - \frac{2r_{doc}}{D_t}\right) \quad (6)$$

We can define the cutting continuity coefficient c as a parameter that measures the relative number of flutes simultaneously in contact with the workpiece and it represents the tool engagement in the workpiece. If it is less than one, the cutting edges do not superpose forces during their cutting, and there is no continuity between cutting forces. It is calculated by:

$$c = \frac{\delta}{\theta_f} + \frac{\theta_{tw}}{\theta_f} \quad (7)$$

as a function of the angle between two flutes $\theta_f = \frac{2\pi}{N_f}$ for N_f flutes.

2.3 Specific Cutting Force

Cutting force models are commonly expressed as a linear function of chip area A_c and specific cutting force [Altintas and Lee, 1996]. The resultant cutting force is predicted by summing the local pressures on cutting edge segments along the flutes. In the present article, specific cutting forces are calculated from the experiments according to the two approaches. One approach is denoted as K_F using average modulus force F^{Av} :

$$K_F = \frac{F^{Av}}{f_t a_{doc}} \quad (8)$$

The second uses the average torque T (N.mm) and is represented by K_T (MPa). It represents the energy used to remove the working material by its volume:

$$K_T = \frac{2000\pi}{60} \frac{Tn}{MRR} \quad (9)$$

The material removal rate MRR (mm^3/s) is calculated using feed velocity on the center of gravity of the removed area and n is the spindle speed (rpm). The thread removed area A_{thr} (Figure 2) is calculated based on thread profile definition and it is written as:

$$A_{thr} = \frac{1}{64} \sqrt{3} P^2 (9 - 16k_t^2) \quad (10)$$

The distance r_{cg} between the center of gravity of the removed area and spindle axis

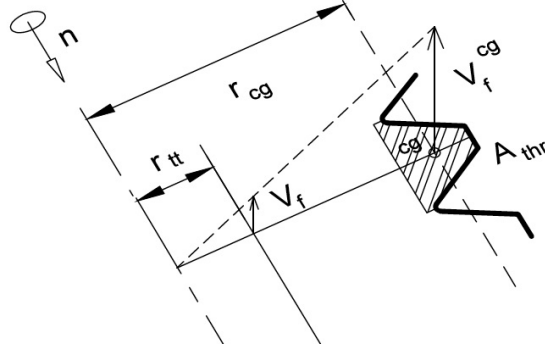


Figure 2: Thread area and feed velocity of the center of gravity

is calculated symbolically as a function of the thread geometry and the expression is presented in Eq. 11:

$$r_{cg} = \frac{(24D(3 + 4k_t) - \sqrt{3}P(27 + 36k_t + 64k_t^2))}{(48(3 + 4k_t))} \quad (11)$$

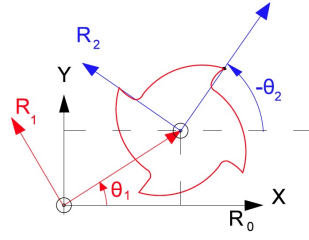
The feed velocity in XY plane of the center of gravity V_f^{cg} (mm/min) is calculated considering the distance r_{cg} .

$$V_f^{cg} = \frac{r_{cg}}{r_{tt}} n N_f f_{t_{xy}} \quad (12)$$

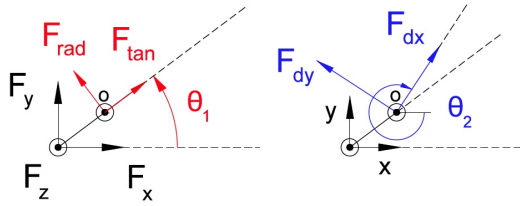
So, the MRR is calculated by the following expression:

$$MRR = \frac{V_f^{cg}}{60} \cdot \frac{A_{thr} \cdot a_{doc}}{P} \quad (13)$$

2.4 Referential Frames



(a) Referential Frames R_0 , R_1 and R_2



(b) Forces Components

Figure 3: Cutting force components in different referential frames.

Three referential frames are important while analyzing the components of thread milling resultant forces: R_0 , R_1 and R_2 , as shown in Figure 3b. The fixed referential R_0 is located in the center of the machined hole oriented by the machine axis. The tool axis coordinates x , y and z and the forces F_x , F_y , F_z are written in R_0 . The tool axis position in XY plane defines $\theta_1 = \arctan(y/x)$ and locates R_1 .

The referential frame R_1 moves with the tool axis while it describes the helical trajectory, as shown in Figure 3b. The local interaction between the tool and the machined surface are described by forces F_{rad} and F_{tan} , radial and tangent to the drilled surface, written in R_1 . The referential frame R_2 is fixed in the tool axis oriented by one fixed point in one cutting edge. Tool rotation angle θ_2 is positive to the clockwise direction. The rotating dynamometer forces F_{dx} , F_{dy} and F_z are measured in the referential frame R_2 .

The resultant cutting force \vec{F} can be decomposed in the described referential frames. Equation 14 is used to transform measured forces in R_2 to the machine-tool frame R_0 ,

$$\vec{F} = \begin{bmatrix} F_x \\ F_y \\ F_z \end{bmatrix} = \begin{bmatrix} \cos(-\theta_2) & -\sin(-\theta_2) & 0 \\ \sin(-\theta_2) & \cos(-\theta_2) & 0 \\ 0 & 0 & 1 \end{bmatrix} \begin{bmatrix} F_{dx} \\ F_{dy} \\ F_z \end{bmatrix}, \quad (14)$$

and equation 15 calculates the force components in R_1 :

$$\vec{F} = \begin{bmatrix} F_{rad} \\ F_{tan} \\ F_z \end{bmatrix} = \begin{bmatrix} \cos(-\theta_1) & -\sin(-\theta_1) & 0 \\ \sin(-\theta_1) & \cos(-\theta_1) & 0 \\ 0 & 0 & 1 \end{bmatrix} \begin{bmatrix} F_y \\ F_x \\ F_z \end{bmatrix}. \quad (15)$$

It should be claimed that the previous articles [Araujo et al., 2006, Sharma et al., 2012] described local cutting forces in local cutting edge referential frames (dF_t and dF_r) which in not the case of this article. Nevertheless, the resultant force can be predicted by integration of local force models.

3 Experimental Procedure

The aim of the experiments is to analyze cutting force components in different referential frames and relate them to the variance of the tests. All experiments were carried out on a CNC machining center DMC85VL. Right hand metric threads were machined in titanium alloy Ti6Al4V workpiece with water based emulsion. A solid carbide coated tool was used for down milling with half penetration strategy.

As feed per tooth proposed by tool supplier used very low chip thickness, a first set of experiments was developed to define feed. A unique thread geometry was machined using one tool and different feed values: from $f_t = 0.02$ up to 0.5 mm/th, when the machine-tool current torque achieve instability. The tool was inspected after each test and the feed range presented in Table 1 was defined.

3.1 Design of Experiments

The design of experiments was developed using five factors: four with two levels and one with three levels. Different designed tools were specially manufactured by Walter Prototyp using two levels for tool orthogonal rake angle γ_{ot} , three levels for flute angle λ_{st} , same radial clearance angle, same tool diameter ($D_t = 10$ mm) and having four flutes. Four different thread geometries were machined: M12x1 and M18x1, with two different axial depth of cut (12 and 18 mm). Drilled diameters and workpiece hardness were controlled to guarantee workpiece homogeneity. Thread milling run-out was measured to assure levels below 0.01 mm. One replica was used for each experiment.

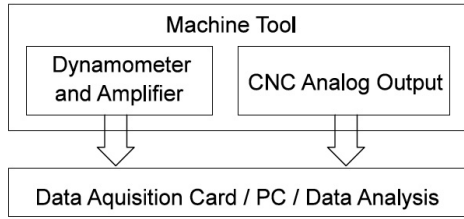
The complete experimental board had 48 experiments using the same cutting speed $V_c = 35$ m/min. Table 1 presents the full design of experiments developed: five basic factors and five composed parameters (A_c , t_{cmax} , δ , MRR and c).

Table 1: Experimental Cutting Parameters and Levels

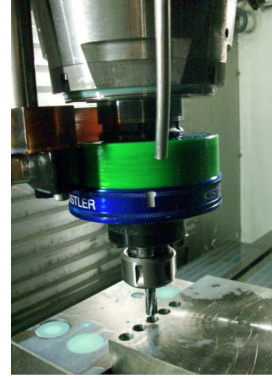
	Basic Factors	Levels
(1)	Rake angle (γ_{nt})	Low (10°) and High (20°)
(2)	Flute angle (λ_{st})	10° , 20° and 30°
(3)	Feed per tooth (f_t)	Low (0.1 mm) and High (0.2 mm)
(4)	Axial depth of cut (a_{doc})	Low (12 mm) and High (18 mm)
(5)	Nominal thread diameter (D)	Low (12 mm) and High (18 mm)
	Composed Factors	Levels
(6)	A_c (function of f_t and a_{doc})	4 levels (1.2; 1.8; 2.4 and 3.6 mm)
(7)	t_{cmax} (function of f_t and D)	4 levels (0.06; 0.09; 0.13 and 0.18 mm)
(8)	δ (function of λ_{st} and a_{doc})	6 Levels (from 24° to 119°)
(9)	MRR (function of f_t , a_{doc} and D)	8 Levels (from 46 to 348 mm^3/min)
(10)	c (function of λ_{st} , a_{doc} and D)	12 Levels (from 0.72 to 2.08)

3.2 Experimental Set-up

The experiments were carried out with continuous data acquisition as shown in Figure 4a. Cutting forces, torque and spindle peak were measured with a Kistler 9123C rotating dynamometer (Figure 4b) and it allowed the determination of θ_2 . The tool was fixed into the holder aligning the cutting edges to the dynamometer axis. Tool axis position (x , y and z) were read from CNC analog output in order to determine θ_1 . All data were digitalized using National Instruments DAC and DasyLab software.



(a) Data Acquisition Set-up



(b) Dynamometer, Tool and Workpiece

Figure 4: Thread Milling Set-up

4 Experimental Results

In order to analyze the thread milling parameters and to have a good comparison between all the experiments, only data in steady state is considered. The steady state is achieved when the tool is not on the region affected by penetration. The tool track during penetration is compared to the inner diameter and the steady state can be found to be from point A to point B in Figure 1a, for the case when $D = 12$ mm. After point B, the tool engages an affected region by the penetration and θ_1 is bigger than 150° . For all data experiments, the same θ_1 range was used to guarantee the same axial depth of cut variation and a proper the comparison of forces.

4.1 Definition of output parameters

Forces were measured in referential frame R_2 and, using x and y information, θ_1 , F_{rad} and F_{tan} in R_1 were calculated, as shown in example of Figure 5. The following forces are analyzed: the average of the resultant force modulus F^{Av} ; the average of radial forces F_{rad}^{Av} ; peak-to-peak of the resultant force modulus F^{PP} ; and peak-to-peak of the radial force F_{rad}^{PP} . The relation F^{PP}/F^{Av} is calculated to quantify the cutting force variation. Complete revolutions are considered for calculating average and peak-to-peak forces. The average specific force is calculated using both approaches:

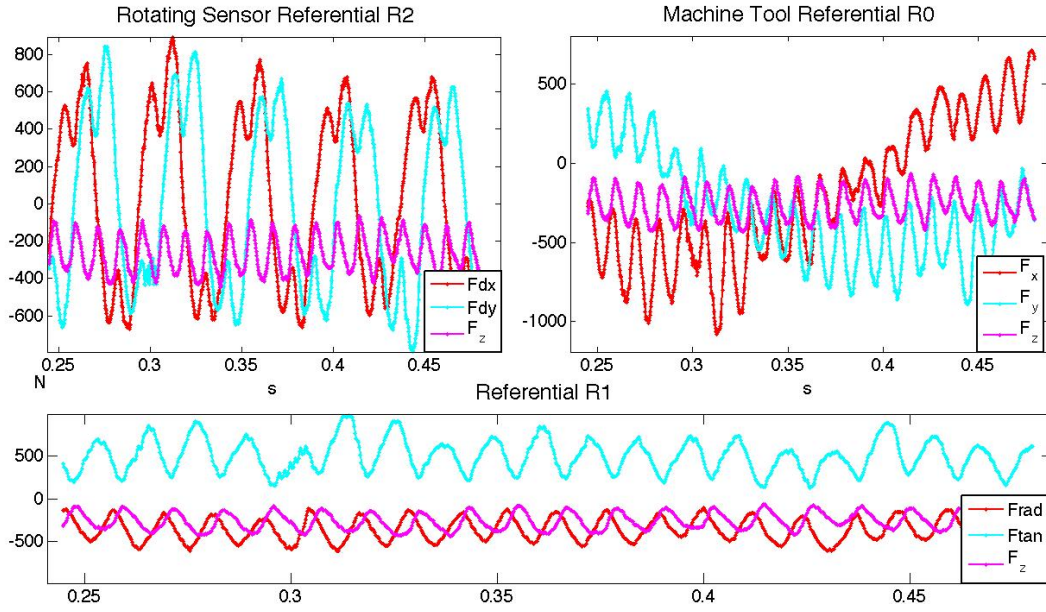


Figure 5: Force components in steady state (N) as a function of time (s) (In this example: feed is 0.2 mm/th, axial depth of cut is 12 mm, the thread diameter is 12 mm, rake angle is 10° , helix angle is 20° and one revolution represents 0.054 s.)

K_F is calculated using resultant forces and K_T is calculated using the experimental torque.

4.2 Analysis of Variance

Analysis of variance (ANOVA) is developed using the representative values presented as output parameters. The effects of the five basic factors and composed factors presented in Table 1 are analyzed using P-value to verify significancy. The ANOVA results are presented in Figures 6, 7 and 8. Figure 6 represents the effects of the basic inputs on specific cutting forces (K_F and K_T) in the upper table, and on average and peak-to-peak resultant force (F^{Av} and F^{PP}) and on average and peak-to-peak radial force (F_{rad}^{Av} and F_{rad}^{PP}) in the lower table. Figure 7 completes the analysis adding significant effects of input parameters interaction and figure 8 presents the significant effects on the percentage of cutting force variation represented by $\frac{F^{PP}}{F^{Av}}$.

5 Discussion

The results presented in Figures 6 to 8 show that the most significant parameter on specific cutting forces are the thread diameter, feed per tooth and the flute angle. It can be seen that flute angle has high impact on forces even though has inverse effect on average and peak-to-peak forces.

Concerning the effect of the thread diameter, it can be claimed, using data from Figure 6, that there is a direct impact in the specific cutting force K_T . That it is because when the thread diameter is bigger, the maximum uncut chip thickness

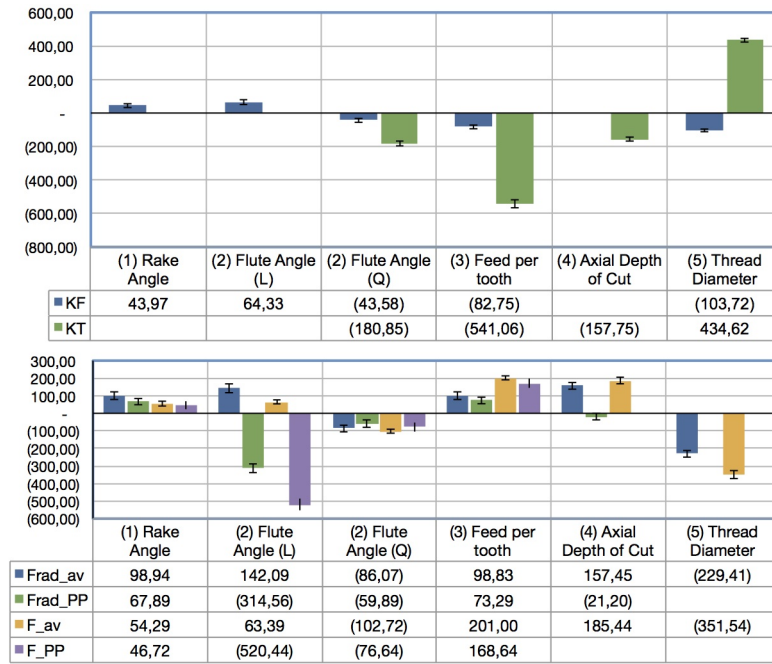


Figure 6: Representative Effects of Basic Parameters on Specific Forces (on the upper bars), Radial and Resultant Average Forces, and Radial and Resultant Peak-to-peak Forces (on lower bars)



Figure 7: Representative Effects of Basic and Interaction Parameters on Specific Forces (on the upper bars), Radial and Resultant Average Forces, and Radial and Resultant Peak-to-peak Forces (on lower bars)

decreases, which it induces higher specific cutting forces explained by mechanical behavior of metal cutting. This relation cannot be analyzed on K_F because its definition does not take into account thread diameter. As the tool diameter D_t is constant for all experiments, the increase of the thread diameter D induces higher pressures on cutting edge and also lower global forces on the tool with positive contribution to reduce tool stress.

The axial depth of cut and feed per tooth has a known effect on average forces, due to the direct relation with cutting area. The feed per tooth impacts directly the average and the peak-to-peak forces, as expected, but it does not represents changes on the relation $\frac{F^{PP}}{F^{Av}}$, as it can be seen in Figure 8. As the feed per tooth is connected to the uncut chip thickness, the specific cutting force is increasing when it decreases, for the same reason as D .

The flute angle factor presented a negative quadratic effect and positive linear effect on the specific cutting forces, and one can suppose that, for this range, lowest flute angle reduces tool stress. Furthermore, higher flute angle induces, along the cutting edge, local values of normal rake angle to be negative [Fromentin and Poulachon, 2010a] and it increases the global forces, as can be seen from Figure 6.

The effect induced by the rake angle γ_{nt} cannot be concluded from these experiments as per the relation with the uncut chip thickness and the honing radius r_β . The measured r_β has 20 microns in average and the experiments range of t_{cmax} where from 60 to 180 microns. In the lower case, the honing radius represents 30% of the tool, and it impacts the average γ_{nt} and it does not happens in the highest case, that represents 9%.

Lower peak-to-peak forces reduce vibration and improve thread quality. Even though there is no significant effect of thread diameter on PP forces, the combined effect of flute angle and thread diameter has important effect on the relation of $\frac{F^{PP}}{F^{Av}}$ shown on Figure 8. The reduction of radial forces avoid tool bending and it contributes for the precision on the thread dimension.

Figure 8 confirms that the cutting continuity coefficient is an important parameter in thread milling. All three parameters that are related to c , which are a_{doc} , λ_{st} and D , shown a important effect on $\frac{F^{PP}}{F^{Av}}$. This variation of this parameter contributes to a variation on PP forces, with negative relation. So, if there is an increase of a_{doc} and λ_{st} or a decrease of D , the PP forces are reduced. If we analyze the two components of c , the first part ($\frac{\delta}{\theta_f}$) includes only the combined parameters a_{doc} with λ_{st} , that are the most influence part, as it is shown in Figure 8. The relation $\frac{\delta}{\theta_f}$, dependent only by D , has not shown much sensibility on $\frac{F^{PP}}{F^{Av}}$.

Force and specific cutting force analysis lead to claim that for this specific case of thread geometry there is an optimization of the flute angle. Figure 9 shows the average value for specific pressure and average forces on the different flute angles, from 10 to 30°. These experiments presented lower force and pressure values for 20° flute angle.

6 Conclusions

This article presents an experimental based work with geometrical analysis for better understanding of effects caused by thread milling geometry, cutting conditions

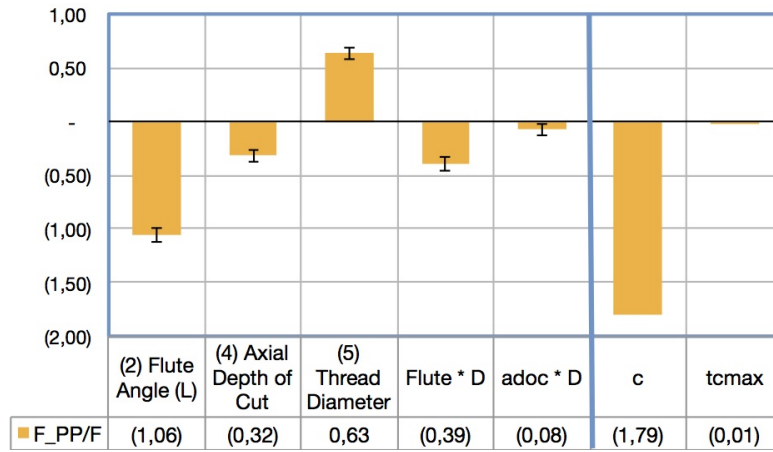


Figure 8: Representative Effects on the Ratio Peak-to-peak Resultant Force Related to the Average Force

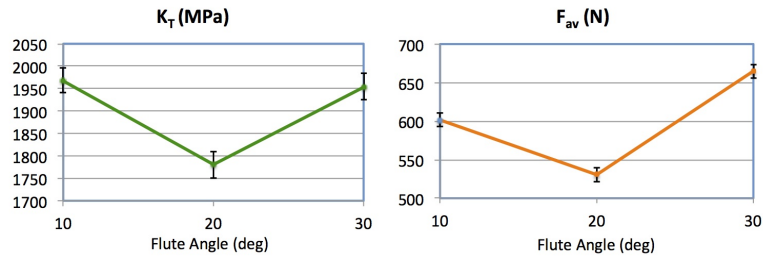


Figure 9: Effect of Flute Angle on Specific Cutting Force (MPa) and Average Resultant Forces (N)

and tool angles on tool forces. Further geometrical and kinematic aspects, data experiments are collected based on a design of experiments using 5 independent variables with 2 and 3 factors and a statistical analysis using ANOVA is applied. Mechanical analysis is developed by considering the material surface orientation using the local referential and it allows the computation of radial and tangential forces to the hole. Also it is presented an interesting experimental setup that measures the rotation angle and the information of the axis position (XYZ on the machine) at the same time of measuring the forces while the machine is executing the machining operation. This data helps to associate the force analysis, the tool engagement and the uncut chip thickness. Previously this was not done on cylindrical milling and thread milling process, when using helical interpolation. The geometrical analysis used on this article proposes new criteria, and also a new reference frame, for explaining cutting force variation. This added reference frame is oriented normally to the hole surface through the tool axis and it gives information about tool deflection. These points are absolutely necessary for cutting force model identification in thread milling.

Based on the methodology applied on the present study, the following conclusions can be claimed:

- (1) Low feed per tooth values induce low uncut chip thickness which can lead to higher cutting pressure on cutting edge. This would be not appropriate for using high flute angle milling cutters which have negative local rake angle.
- (2) The average resultant forces is linked to cutting conditions and also to tool geometry used. This study shows that it exists an optimized flute angle to reduce the resultant forces. In the present case, for the used thread dimension, the optimum flute angle is near 20° .
- (3) The geometrical analysis allows to define significant criteria. The cutting continuity coefficient is clearly correlated to the cutting force variation, represented by the ratio peak-to-peak resultant force related to the average force.
- (4) This study propose a contribution of the understanding of geometrical and mechanical aspects in thread milling. Further contribution would develop realistic mechanical model with taking into account local parameters to reproduce the behavior of metal cutting by thread milling.

Acknowledgement

The authors would like to gratefully acknowledge the Walter Prototyp tool manufacturer who specially machined the requested tools. The first author would like to thanks the support of BRAFITEC/CAPES and the research team in LABOMAP at Arts et Metiers ParisTech.

References

[ISO, 1998] (1998). Iso general purpose screw threads basic profile part 1 metric screw threads. *ISO Standard*, 68(1):82 – 88.

- [Altintas and Lee, 1996] Altintas, Y. and Lee, P. (1996). A general mechanics and dynamics model for helical end mills. *CIRP Annals - Manufacturing Technology*, 45(1):59 – 64.
- [Araujo and Jun, 2009] Araujo, A. C. and Jun, M. B. (2009). The specific cutting energy on the cutting edges of a combined drilling/thread milling process: Thrilling. *12th CIRP Conference on Modelling of Machining Operations*.
- [Araujo et al., 2006] Araujo, A. C., Silveira, J. L., Jun, M. B., Kapoor, S. G., and DeVor, R. (2006). A model for thread milling cutting forces. *International Journal of Machine Tools and Manufacture*, 46(15):2057 – 2065.
- [Araujo et al., 2004] Araujo, A. C., Silveira, J. L., and Kapoor, S. G. (2004). Force prediction in thread milling. *J. of the Braz. Soc. of Mech. Sci. and Eng.*, XXVI(1):82 – 88.
- [Armarego and Chen, 2002] Armarego, E. and Chen, M. N. (2002). Predictive cutting models for the forces and torque in machine tapping with straight flute taps. *CIRP Annals - Manufacturing Technology*, 51(1):75 – 78.
- [Cao and Sutherland, 2002] Cao, T. and Sutherland, J. W. (2002). Investigation of thread tapping load characteristics through mechanistics modeling and experimentation. *International Journal of Machine Tools and Manufacture*, 42(14):1527 – 1538.
- [Fromentin and Poulachon, 2010a] Fromentin, G. and Poulachon, G. (2010a). Geometrical analysis of thread milling—part 1: evaluation of tool angles. *The International Journal of Advanced Manufacturing Technology*, 49(1):73–80.
- [Fromentin and Poulachon, 2010b] Fromentin, G. and Poulachon, G. (2010b). Geometrical analysis of thread milling—part 2: calculation of uncut chip thickness. *The International Journal of Advanced Manufacturing Technology*, 49(1):81–87.
- [Fromentin et al., 2005] Fromentin, G., Poulachon, G., Moisan, A., Julien, B., and Giessler, J. (2005). Precision and surface integrity of threads obtained by form tapping. *CIRP Annals - Manufacturing Technology*, 54(1):519 – 522.
- [Fromentin et al., 2011] Fromentin, G., Sharma, V., Poulachon, G., Paire, Y., and Brendlen, R. (2011). Effect of thread milling penetration strategies on the dimensional accuracy. *Journal of Manufacturing Science and Engineering*, 133(4).
- [Ghani et al., 2004] Ghani, J., Choudhury, I., and Hassan, H. (2004). Application of taguchi method in the optimization of end milling parameters. *Journal of Materials Processing Technology*, 145(1):84 – 92.
- [Li et al., 2003] Li, W., Li, D., and Ni, J. (2003). Diagnosis of tapping process using spindle motor current. *International Journal of Machine Tools and Manufacture*, 43(1):73 – 79.
- [Lopez-Heredia et al., 2008] Lopez-Heredia, M., Goyenvalle, E., Aguado, E., Pilet, P., Leroux, C., Dorget, M., P, P. W., and Layrolle, P. (2008). Bone growth in rapid prototyped porous titanium implants. *J Biomed Mater Res A*, 85(3):664–673.

- [Malaguti et al., 2011] Malaguti, G., Denti, L., Bassoli, E., Franchi, I., Bortolini, S., and Gatto, A. (2011). Dimensional tolerances and assembly accuracy of dental implants and machined versus cast-on abutments. *Clin Implant Dent Relat Res*, 13(2):134–40.
- [Mezentsev et al., 2002] Mezentsev, O. A., Zhu, R., DeVor, R. E., Kapoor, S. G., and Kline, W. A. (2002). Use of radial forces for fault detection in tapping. *International Journal of Machine Tools and Manufacture*, 42(4):479 – 488.
- [Sharma et al., 2012] Sharma, V., Fromentin, G., and Poulachon, G. (2012). Investigation of cutting tool geometry effect on cutting forces during thread milling. *Submitted for publication at the Journal of Manufacturing Science and Technology - CIRP*, pages 1– 10.
- [Thusty and MacNeil, 1975] Thusty, J. and MacNeil, P. (1975). Dynamics of cutting forces in end milling. *Annals of the CIRP*, 24:2125.
- [Veldhuis et al., 2007] Veldhuis, S., Dosbaeva, G., and Benga, G. (2007). Application of ultra-thin fluorine-content lubricating films to reduce tool/workpiece adhesive interaction during thread-cutting operations. *International Journal of Machine Tools and Manufacture*, 47(34):521 – 528.
- [Yamazoe, 2010] Yamazoe, M. (2010). Study of corrosion of combinations of titanium/ti-6al-4v implants and dental alloys. *Dent Mater J*, 29(5):542–553.
- [Yang et al., 2009] Yang, Y.-K., Chuang, M.-T., and Lin, S.-S. (2009). Optimization of dry machining parameters for high-purity graphite in end milling process via design of experiments methods. *Journal of Materials Processing Technology*, 209(9):4395 – 4400.